The Journal of Physiology

Distinct cytoprotective roles of pyruvate and ATP by glucose metabolism on epithelial necroptosis and crypt proliferation in ischaemic gut

Ching-Ying Huang[1], Wei-Ting Kuo[1], Chung-Yen Huang[1], Tsung-Chun Lee[1,2], Chin-Tin Chen[3], Wei-Hao Peng[4], Kuo-Shyan Lu[4], Chung-Yi Yang[5,6] and Linda Chia-Hui Yu[1]

[1] *Graduate Institute of Physiology, National Taiwan University College of Medicine, Taipei, Taiwan*
[2] *Department of Internal Medicine, National Taiwan University Hospital, Taipei, Taiwan*
[3] *Department of Biochemical Science and Technology, National Taiwan University, Taipei, Taiwan*
[4] *Graduate Institute of Anatomy and Cell Biology, National Taiwan University College of Medicine, Taipei, Taiwan*
[5] *Department of Medical Imaging, E-Da Hospital, I-Shou University, Kaohsiung, Taiwan*
[6] *Department of Medical Imaging, National Taiwan University Hospital, Taipei, Taiwan*

Key points

- Intestinal ischaemia causes epithelial death and crypt dysfunction, leading to barrier defects and gut bacteria-derived septic complications.
- Enteral glucose protects against ischaemic injury; however, the roles played by glucose metabolites such as pyruvate and ATP on epithelial death and crypt dysfunction remain elusive.
- A novel form of necrotic death that involves the assembly and phosphorylation of receptor interacting protein kinase 1/3 complex was found in ischaemic enterocytes.
- Pyruvate suppressed epithelial cell death in an ATP-independent manner and failed to maintain crypt function. Conversely, replenishment of ATP partly restored crypt proliferation but had no effect on epithelial necroptosis in ischaemic gut.
- Our data argue against the traditional view of ATP as the main cytoprotective factor by glucose metabolism, and indicate a novel anti-necroptotic role of glycolytic pyruvate under ischaemic stress.

Abstract Mesenteric ischaemia/reperfusion induces epithelial death in both forms of apoptosis and necrosis, leading to villus denudation and gut barrier damage. It remains unclear whether programmed cell necrosis [i.e. receptor-interacting protein kinase (RIP)-dependent necroptosis] is involved in ischaemic injury. Previous studies have demonstrated that enteral glucose uptake by sodium-glucose transporter 1 ameliorated ischaemia/reperfusion-induced epithelial injury, partly via anti-apoptotic signalling and maintenance of crypt proliferation. Glucose metabolism is generally assumed to be cytoprotective; however, the roles played by glucose metabolites (e.g. pyruvate and ATP) on epithelial cell death and crypt dysfunction remain elusive. The present study aimed to investigate the cytoprotective effects exerted by distinct glycolytic metabolites in ischaemic gut. Wistar rats subjected to mesenteric ischaemia were enterally instilled glucose, pyruvate or liposomal ATP. The results showed that intestinal ischaemia caused RIP1-dependent epithelial necroptosis and villus destruction accompanied by a reduction in crypt proliferation. Enteral glucose uptake decreased epithelial cell death and increased crypt proliferation, and ameliorated mucosal histological damage. Instillation of cell-permeable pyruvate suppressed epithelial cell death in an ATP-independent manner and improved the villus morphology but failed to maintain crypt function. Conversely, the administration of liposomal ATP partly restored crypt proliferation but did not reduce epithelial necroptosis and histopathological injury. Lastly,

 DOI: 10.1113/JP272208

glucose and pyruvate attenuated mucosal-to-serosal macromolecular flux and prevented enteric bacterial translocation upon blood reperfusion. In conclusion, glucose metabolites protect against ischaemic injury through distinct modes and sites, including inhibition of epithelial necroptosis by pyruvate and the promotion of crypt proliferation by ATP.

(Received 27 January 2016; accepted after revision 24 March 2016; first published online 28 April 2016)
Corresponding author L. C.-H. Yu: Graduate Institute of Physiology, National Taiwan University College of Medicine, Suite 1020, #1 Jen-Ai Rd. Sec. I, Taipei 100, Taiwan. Email: lchyu@ntu.edu.tw

Abbreviations CFU, colony forming unit; Gd, gadodiamide; GLUT2, glucose transporter 2; I/R, ischaemia/reperfusion; Isch, ischaemia; MRI, magnetic resonance imaging; Nec1, necrostatin-1; NF-κB, nuclear factor-kappa B; 3-OMG, 3-*O*-methyl-glucopyranoside; PCNA, proliferating cell nuclear antigen; PI3K, phosphatidylinositol 3-kinase; RIP, receptor interacting protein kinase; SGLT1, sodium/glucose transporter 1; SMA, superior mesenteric artery; TUNEL, terminal deoxynucleotidyl transferase dUTP-biotin nick end labelling; Veh, vehicle.

Introduction

Intestinal ischaemia/reperfusion (I/R) injury is a pathological condition seen in clinical cases of necrotizing enterocolitis, mesenteric artery embolism, and traumatic and haemorrhagic shock, as well as in patients undergoing major cardiovascular and abdominal surgery (Debus *et al.* 2011; Eltzschig *et al.* 2014). Enteric bacterial translocation and septic complications are observed following epithelial barrier damage in mesenteric I/R insults (Hsiao *et al.* 2009). At the cellular level, metabolic and oxidative stresses are caused by ischaemia as a result of a loss of oxygen and nutrient supply, and are exacerbated by a burst of free radicals upon blood reperfusion (Vanlangenakker *et al.* 2008). Both types of epithelial cell death (i.e. apoptosis and necrosis) accompanied by villous tip sloughing and crypt dysfunction were documented in mesenteric I/R (Shah *et al.* 1997; Little *et al.* 2003; Azuara *et al.* 2005; Huang *et al.* 2011).

Although key regulating proteins for epithelial apoptosis and anti-apoptotic signalling have been studied extensively (Huang *et al.* 2011; Cheng *et al.* 2013; Schulz *et al.* 2013), there is an apparent lack of knowledge on the molecular machinery for cell necrosis and anti-necrotic factors upon ischaemic challenge. Necrosis has been traditionally considered as an unregulated form of cell death characterized by mitochondrial swelling, sub-cellular organelle breakdown and plasma membrane explosion. An alternative form of programmed cell necrosis, termed necroptosis, was recently identified that involves phosphorylation and complex formation of receptor-interacting protein (RIP)1/3 and mitochondrial free radical synthesis (Temkin *et al.* 2006; Cho *et al.* 2009; Declercq *et al.* 2009; He *et al.* 2009; Zhang *et al.* 2009). RIP1/3-mediated necroptosis in intestinal epithelial cells has been documented in murine models of experimental enterocolitis and in patients with inflammatory bowel disease (Gunther *et al.* 2011; Welz *et al.* 2011; Pierdomenico *et al.* 2014), as well as in *in vitro* epithelial cell cultures exposed to hypoxic stress or cytotoxic stimulation (Chakrabarti *et al.* 2003; Kalischuk *et al.* 2007; Huang *et al.* 2013). Recently, necroptosis was reported in ischaemic brain, kidney and heart models (Liang *et al.* 2014; Luedde *et al.* 2014; Yin *et al.* 2015). It remains unclear whether RIP signals are involved in mechanisms of intestinal ischaemia-induced epithelial necrosis and whether cytoprotective pathways exist to inhibit necroptosis in the gut.

Dual routes of nutrient supply (haematologic and dietary sources) and dynamic epithelial restitution along the crypt–villus axis are unique characteristics of the intestinal tract. Previous studies have demonstrated that glucose uptake inhibited morphological injury and epithelial apoptosis caused by mesenteric I/R (Kozar *et al.* 2002; Huang *et al.* 2011) and repressed cell necroptosis triggered by hypoxia (Huang *et al.* 2013). Moreover, glucose supplementation also prevented the loss of crypt proliferation following I/R insults (Huang *et al.* 2011). Although gut protection by glucose has been generally assumed to be related to energy replenishment, other mechanisms were identified, such as activation of anti-apoptotic phosphatidylinositol 3-kinase (PI3K)/Akt and nuclear factor-kappa B (NF-κB) signals, as well as scavenging of mitochondrial oxidative free radicals by glucose metabolites (Yu *et al.* 2005; Palazzo *et al.* 2008; Yu *et al.* 2008; Huang *et al.* 2011; Huang *et al.* 2013). Intracellular glucose undergoes anaerobic glycolysis to generate pyruvate that feeds into the tricarboxylic acid cycle in mitochondrial respiration for oxygen-dependent energy production (Fleming *et al.* 1997; Fink, 2010). Pyruvate *per se* also acts as a free radical scavenger via non-enzymatic reactions and inhibits I/R-induced mucosal injury (Cicalese *et al.* 1996; Sims *et al.* 2001; Fink, 2010; Kao & Fink, 2010). To date, the protective roles of glucose metabolites (i.e. pyruvate and ATP) on epithelial cell death and crypt dysfunction in ischaemic tissues remain incompletely understood.

The present study aimed to investigate whether RIP-dependent necroptosis are involved in ischaemia-induced mucosal injury and whether enteral glucose uptake

protects against epithelial cell death and restores crypt proliferation via distinct metabolic products.

Methods

Animal models of intestinal ischaemia (Isch) and ischaemia/reperfusion (I/R)

All animal protocols used in the present study were approved and monitored by the Institutional Animal Care and Use Committee in National Taiwan University. Male Wistar rats (250–300 g) were fasted overnight with free access to water and subjected to sham operation, mesenteric Isch or I/R challenge as described previously (Hsiao *et al.* 2009; Huang *et al.* 2011; Lu *et al.* 2012). After anaesthetization with urethane (1.2 g kg^{-1}, I.P.; Sigma, St Louis, MO, USA) and confirmation with a lack of toe withdrawal reflex in each animal, rats were subjected to midline laparotomy. Isch rats were subjected to occlusion of the superior mesenteric artery (SMA) with an atraumatic microvascular clamp for 20 min and killed. In I/R rats, the clamp was then released for 60 min before death. Sham-operated control rats received mock manipulation of SMA and were killed after the same period of time. The anaesthesia and surgical procedures comply with the animal ethics checklist of with *The Journal of Physiology*.

Experimental design

The surgical procedures were carried out under aseptic conditions. After anaesthetization, a 10 cm jejunal sac was created by thread ligature at both ends, beginning 10 cm distal to the ligament of Treitz in each animal as described previously (Hsiao *et al.* 2009; Huang *et al.* 2011). A 1 mL syringe with a PE-10 catheter was intubated to one end of the jejunal sac and 0.5 mL of Krebs buffer with the following substances (see below) was carefully injected into the lumen. Animals were then subjected to sham operation, Isch, or I/R as stated above.

In the first set of experiments investigating epithelial necrosis by mesenteric ischaemia, rats were randomly assigned to four groups ($n = 6$–8 per group): Group 1, 'CON + Veh' rats that underwent laparotomy and whose jejunal lumen was instilled with Krebs buffer vehicle (Veh) before sham operation; Group 2, 'CON + Nec1' rats that were enterally administered 500 μM necrostatin-1 (Nec1, a specific RIP1 inhibitor) in Krebs buffer 20 min before sham operation; Group 3, 'Isch + Veh' rats that were enterally instilled with Krebs buffer before SMA occlusion for 20 min; and Group 4: 'Isch + Nec1' rats that were enterally administered 500 μM Nec1 in Krebs buffer immediately before SMA occlusion for 20 min.

In the second set of experiments, Isch rats were enterally given 25 mM of glucose or cell-permeable ethyl pyruvate (Huang *et al.* 2013) in the absence or presence of glucose transporter inhibitors in the jejunal sac. An sodium/glucose transporter 1 (SGLT1) inhibitor phloridzin (2.5 mM) or a glucose transporter 2 (GLUT2) inhibitor phloretin (2.5 mM) was added to the glucose solution to confirm the transporter involved. Additionally, Isch rats were enterally administered empty liposomes or ATP-encapsulated liposomes synthesized by Dr Chin-Tin Chen (Peng *et al.* 2015). The concentration of ATP loaded in liposomes was 6.6 mM, as determined by using a commercial ATP assay kit (Invitrogen, Grand Island, NY, USA). All reagents were purchased from Sigma, except the lipids, which were purchased from Avanti Polar Lipids (Birmingham, AL, USA).

In the next set of experiments, rats were subjected to sham-operation (Sham) and I/R challenge with or without enteral glucose or pyruvate (25 mM). In some groups, enteral glucose was replaced by equimolar concentrations of 3-*O*-methyl-glucopyranoside (3-OMG; a non-metabolizable sugar analogue taken up by glucose transporters), mannitol (a non-absorbable and non-metabolizable sugar used as an osmolarity control) or glutamate (an amino acid used as an oxidative fuel control) before I/R challenge. All reagents were purchased from Sigma.

Measurement of pyruvate and ATP contents

Intestinal segments were excised and luminal contents gently rinsed off. Scraped mucosal lysates were used for the assessment of intracellular pyruvate (Biovision, Milpitas, CA, USA) and ATP levels (Invitrogen) using commercial assay kits in accordance with the manufacturer's instruction (Huang *et al.* 2013).

Histopathological scoring

Jejunal segments were fixed in 4% paraformaldehyde and processed for paraffin embedding, and sections of 4 μM thickness were stained with haematoxylin and eosin. The degree of intestinal injury was evaluated using a light microscope and graded by two independent blinded observers based on a previously established scoring system (Huang *et al.* 2011; Lu *et al.* 2012).

Immunoprecipitation of RIP1-RIP3 complex and the *in vitro* kinase assay

Scraped jejunal mucosa was homogenized in ice-cold complete RIPA buffer [1% Nonidet P-40, 0.25% sodium deoxycholate, 10 mM NaF, 5 mM Na_3VO_5, 1 mM phenylmethanesulphonyl fluoride and one tablet of Complete-Mini protease inhibitors cocktail (Roche, Penzberg, Germany) added to 7 ml of buffer immediately before use]. The lysates were centrifuged at 14,000 *g*

for 10 min and the protein concentration of the supernatant was adjusted to 5 mg ml^{-1}. After pre-cleaning with recombinant protein G agarose beads (Invitrogen), the RIP1 protein was immunoprecipitated with anti-human RIP1 (BD Bioscience, Franklin Lakes, NJ, USA) overnight at 4°C. The protein-antibody complexes were then incubated with protein G agarose beads for 1 h at 4°C followed by centrifugation at 14,000 *g* at 4°C and washing with lysis buffer twice. The pellet was dissolved in 2 × electrophoresis sample buffer containing 2% (w/v) SDS, 100 mM dithithreitol and 62.5 mM Tris/HCl (pH 6.8) at a ratio of 1:1, and subjected to 95°C in a heat block for 5 min for denaturation. Samples were used for immunoblotting of RIP3.

The immune complexes were subjected to reducing SDS-PAGE (4-10% polyacrylamide). The resolved proteins were then electroblotted onto Hybond-P polyvinylidene fluoride membranes (Amersham Biosciences, Piscataway, NJ, USA). After blocking for 1 h at room temperature in 5% non-fat dry milk, the membranes were incubated with anti-RIP1 (1:1000; BD Bioscience) or polyclonal rabbit anti-RIP3 (1:1000; Abcam, Cambridge, UK) as the primary antibody overnight. Membranes were washed twice with Tris-buffered saline with 0.1% Tween 20 for 5 min, and incubated with secondary goat anti-rabbit or anti-mouse IgG conjugated with horseradish peroxidase (1:1000; Cell Signaling, Denver, MA, USA) at room temperature for 1 h. The antigens were revealed and the band density was quantified by photoimaging analysis (Huang *et al.* 2013).

Scraped mucosa to be processed for *in vitro* kinase assays were lysed with kinase lysis buffer (20 mM Hepes, 150 mM NaCl, 1% Triton X-100, 5 mM EDTA, 5 mM NaF, 0.2 mM Na_3VO_4, 1 mM phenylmethanesulphonyl fluoride and Complete-Mini protease inhibitors cocktail) followed by immunoprecipitation by anti-RIP1-conjugated beads as described above. The bead pellets were then incubated in kinase reaction buffer (20 mM Hepes, 5 mM $MgCl_2$ and 5 mM $MnCl_2$) supplemented with 10 μM cold ATP and 1 μCi γ-^{32}P-ATP for 30 min at 30°C. The reaction was terminated by adding the same volume of 2 × SDS sample buffer and heat denaturation at 95°C for 5 min, followed by vortex and centrifugation. Samples were resolved on 4–8% SDS-PAGE and exposed to autoradiographic films as described previously (Huang *et al.* 2013).

Terminal deoxynucleotidyl transferase dUTP-biotin nick end labelling (TUNEL) staining

Intestinal tissues fixed in 4% paraformaldehyde was sectioned for TUNEL by using a DNA fragmentation detection kit (Merck, Darmstadt, Germany) (Wu *et al.* 2011; Kuo *et al.* 2015). The percentage of TUNEL-positive epithelial cells per villus was calculated from 10 sections from each animal group.

Ussing chamber study

Muscle-stripped intestinal segments were mounted in Ussing chambers (WPI Instruments, Sarasota, FL, USA) for measurement of electrophysiological values including potential difference (PD), short-circuit current (I_{sc}) and tissue conductance as described previously (Huang *et al.* 2011; Chen *et al.* 2013).

Transmission electron microscopy

Intestinal tissues were fixed in 2% glutaraldehyde and 2% paraformaldehyde in 0.1 M sodium cacodylate buffer (pH 7.4) for 6–8 h at 4°C. After washing in the buffer, tissues were impregnated with 1% osmium teraoxide for 1 h, dehydrated through a graded series of ethanol, and embedded in epoxy resin. Thin sections (70 nm) were cut, stained with uranyl acetate and lead citrate, and examined using an electron microscope (model 7100; Hitach, Tokyo, Japan) equipped with a digital system at 80 kv (Wu *et al.* 2014; Yu *et al.* 2014).

Immunohistochemical and immunofluorescence staining

Intestinal tissue sections for immunostaining were processed as described previously (Huang *et al.* 2011; Kuo *et al.* 2015). Briefly, tissue sections were blocked with 2% normal goat serum, and incubated with primary antibodies to proliferating cell nuclear antigen (PCNA) (dilution 1:100; Lifespan Biosciences, Seattle, WA, USA), Ki67 (dilution 1:100; Abcam, Cambridge, UK) or isotype controls. After washing with phosphate-buffered saline, tissues stained for PCNA were incubated with horseradish peroxidase-conjugated anti-rabbit IHC detection reagent (Cell Signaling) and developed with a 3,3′-diaminobenzidine peroxidase substrate followed by counterstaining with haematoxylin. For Ki67 staining, tissues were incubated with Alexa 488-conjugated secondary antibodies (dilution 1:1000; Invitrogen) and stained with a Hoechst dye to visualize cell nuclei. The slides were mounted with aqueous mounting media and viewed under a fluorescence microscope (Carl Zeiss, Oberkochen, Germany).

To quantify cell proliferation in intestinal tissues, the numbers of Ki67-positive cells per crypt were calculated from 18–25 well-oriented crypts in longitudinal view from each animal and a total of six rats per group were used.

Fluorescein-based gut permeability assay

The 4 kDa fluorescein isothiocyanate-conjugated dextran (FD4; Sigma) dissolved in Krebs buffer was administered into the lumen of ligated jejunal sac to a final concentration of 0.5 mg ml^{-1} immediately after the release of the artery

clamp, and arterial plasma from 0.5 ml of blood was taken at 60 min post-reperfusion as described previously (Huang *et al.* 2011).

Magnetic resonance imaging (MRI)-based gut permeability assay

To assess real-time gut permeability *in vivo*, the contrast agent gadodiamide (Gd; Omniscan; GE Healthcare, Little Chalfont, UK) was instilled into the lumen of the ligated jejunal sac to a final concentration of 0.25 M immediately after the release of the artery clamp, and the signal intensity of this agent in the liver and plasma was quantified using MRI as described previously (Hsiao *et al.* 2009; Huang *et al.* 2011).

Analysis of bacterial translocation

The liver and spleen tissues were homogenized, sonicated and adjusted to a protein concentration of 0.1 g ml^{-1} with sterile phosphate-buffered saline. Each homogenate was inoculated onto fresh blood agar plates (200 μl per plate; Scientific Biotech Corp., Taipei, Taiwan) and the plates were incubated at 37°C overnight. The number of bacterial colony forming units was normalized per gramme of tissue [(colony forming unit) CFU g^{-1}] (Hsiao *et al.* 2009; Huang *et al.* 2011).

Statistical analysis

All values except for bacterial CFU g^{-1} were expressed as the mean ± SEM and the means were compared by one-way analysis of variance followed by a Student–Newman–Keul test. For the bacterial translocation data, pairwise ranking of the median of CFU g^{-1} values was conducted using the non-parametric Mann–Whitney U test. $P < 0.05$ was considered statistically significant.

Results

Mesenteric ischaemia caused RIP-dependent necroptosis in intestinal epithelial cells

Previous studies have reported epithelial apoptosis and villus denudation in I/R rat intestines (Huang *et al.* 2011; Lu *et al.* 2012). To investigate necroptotic signals on the epithelium-covered villus surface, mucosal tissues were collected immediately following mesenteric ischaemia for 20 min. Moreover, Nec1 (a specific RIP1 inhibitor) or vehicle were administered prior to Isch challenge to examine the role of RIP signalling. Formation of RIP1-RIP3 complex and phosphorylation of RIP1 were observed in the jejunal mucosa of Isch rats, as indicated by immunoprecipitation blotting and ^{32}P kinase radioassays (Fig. 1*A*). Necrotic features of jejunal mucosa and an increased histopathological score were observed in Isch rats compared to control groups (Fig. 1*B* and 1*C*). Administration of Nec1 alleviated the villus necrotic features and decreased the histopathology score of ischaemic tissues (Fig. 1*B* and 1*C*).

Mesenteric ischaemia also reduced the PD and I_{sc} of jejunal tissues, and resulted in the trend for an increase in tissue conductance (Fig. 1*D*–*F*). Administration of Nec1 partly restored the PD and I_{sc} to baseline levels but did not decrease tissue conductance (Fig. 1*D*–*F*).

Electromicroscopic imaging revealed an abnormal cellular morphology and enlarged subepithelial spaces of ischaemic enterocytes, in marked contrast to the normal columnar epithelial cells with a highly ordered brush border in control tissues (Fig. 2*A*). Sub-cellular necrotic features and organelle destruction were observed, including mitochondrial swelling, cytoplasmic vacuolation, microvilli in microsomal shapes and plasma membrane disintegration (Fig. 2*B*–*D*). In enterocytes of Isch rats administered with Nec1, no sign of sub-cellular organelle damage was observed and the cellular morphology was comparable to that of normal controls (Fig. 2*A* and 2*B*).

Enteral glucose uptake prevented ischaemia-induced epithelial necroptosis

Our previous study had shown that enteral glucose instillation protected against epithelial cell apoptosis in I/R intestine (Huang *et al.* 2011). In the present study, we examined whether glucose uptake prevents RIP-dependent necroptotic death in enterocytes of Isch rats. Enteral instillation of glucose ablated mucosal RIP1/RIP3 complex formation and RIP1 phosphorylation (Fig. 3*A*) and alleviated villous necrotic features and histopathological damage in ischaemic tissues (Fig. 3*C* and 3*D*).

SGLT1 is the main apical transporter for dietary glucose, whereas GLUT2 is responsible for basolateral diffusion of glucose into the bloodstream (Scheepers *et al.* 2004). To identify the glucose transporters involved in cytoprotection, specific inhibitors were added into the glucose solution during ischaemic challenge. SGLT1-sensitive phloridzin blocked the glucose protection against morphological damage in intestinal mucosa, whereas GLUT2-sensitive phloretin had no effect (Fig. 3*C* and 3*D*).

Glycolytic pyruvate attenuated epithelial cell death in an energy-independent manner

To further clarify the glucose metabolites involved in cyto-protection against ischaemic injury, ATP and pyruvate content in mucosal tissues of Isch rats was quantified. A

significant reduction of mucosal ATP and pyruvate levels was seen in ischaemic tissues compared to controls. Enteral instillation of glucose prevented the drop of both ATP and pyruvate levels in mucosal tissues (Fig. 3*E* and 3*F*).

Because pyruvate and ATP are both final glycolytic products and none of the available inhibitors to glycolytic enzymes are able to differentiate between the synthesis of two substances, blockade studies to the metabolic pathways were not applied in our experimental design. Instead, a cell-permeable pyruvate (ethyl pyruvate) was instilled into the intestinal lumen in an equimolar concentration in place of glucose to confirm its cytoprotective role in Isch rats. Our results showed that pyruvate instillation attenuated RIP1/3-dependent

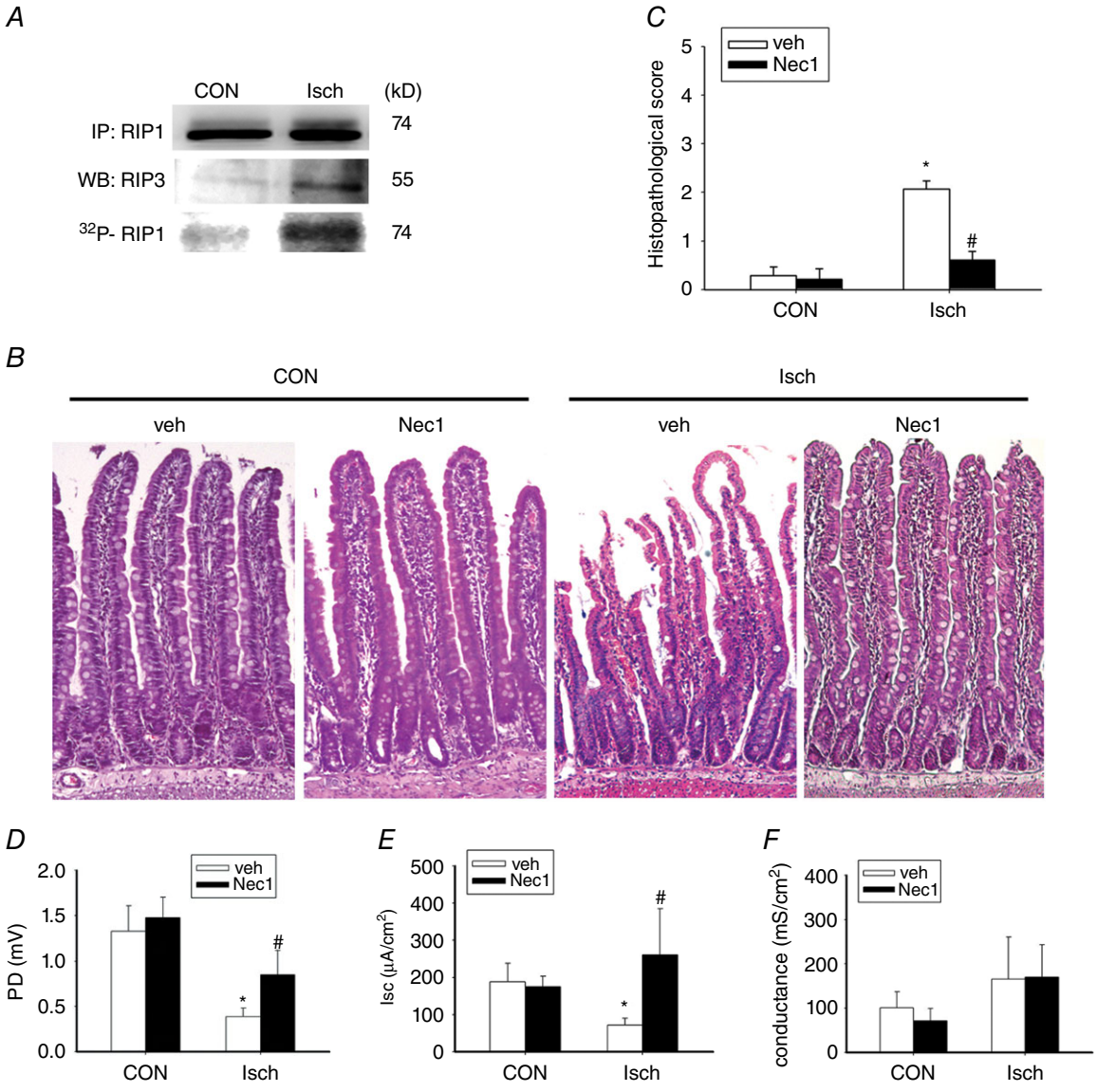

Figure 1. Mesenteric ischaemia caused RIP-dependent necrotic death and histological damage in intestinal mucosa
Isch rats were subjected to occlusion of the superior mesenteric artery for 20 min with or without inhibitors, and jejunal mucosal tissues were collected immediately. *A*, immunoprecipitation blotting showed the formation of RIP1-RIP3 complex and phosphorylation of RIP1 in the jejunal mucosa of Isch rats but not control (CON) rats. The experiments were repeated twice and similar results were obtained ($n = 3$ per group). *B*, histological images of jejunal mucosa in CON and Isch rats administered Nec1 (a specific RIP1 inhibitor). In comparison with normal control tissues, enlargement of the subepithelial space and epithelial denudation were observed at the villous tips of Isch rats. Administration of Nec1 alleviated the ischaemia-induced mucosal histopathology. Magnification 200×. *C*, histopathological scores in the jejunal tissues of CON and Isch rats administered Nec1. The electrophysiological values were examined in intestinal segments, including PD (*D*), I_{sc} (*E*) and tissue conductance (*F*). $^{*}P < 0.05$ *vs.* respective CON, $^{\#}P < 0.05$ *vs.* 'Isch + Veh' ($n = 6$ per group). [Colour figure can be viewed at wileyonlinelibrary.com]

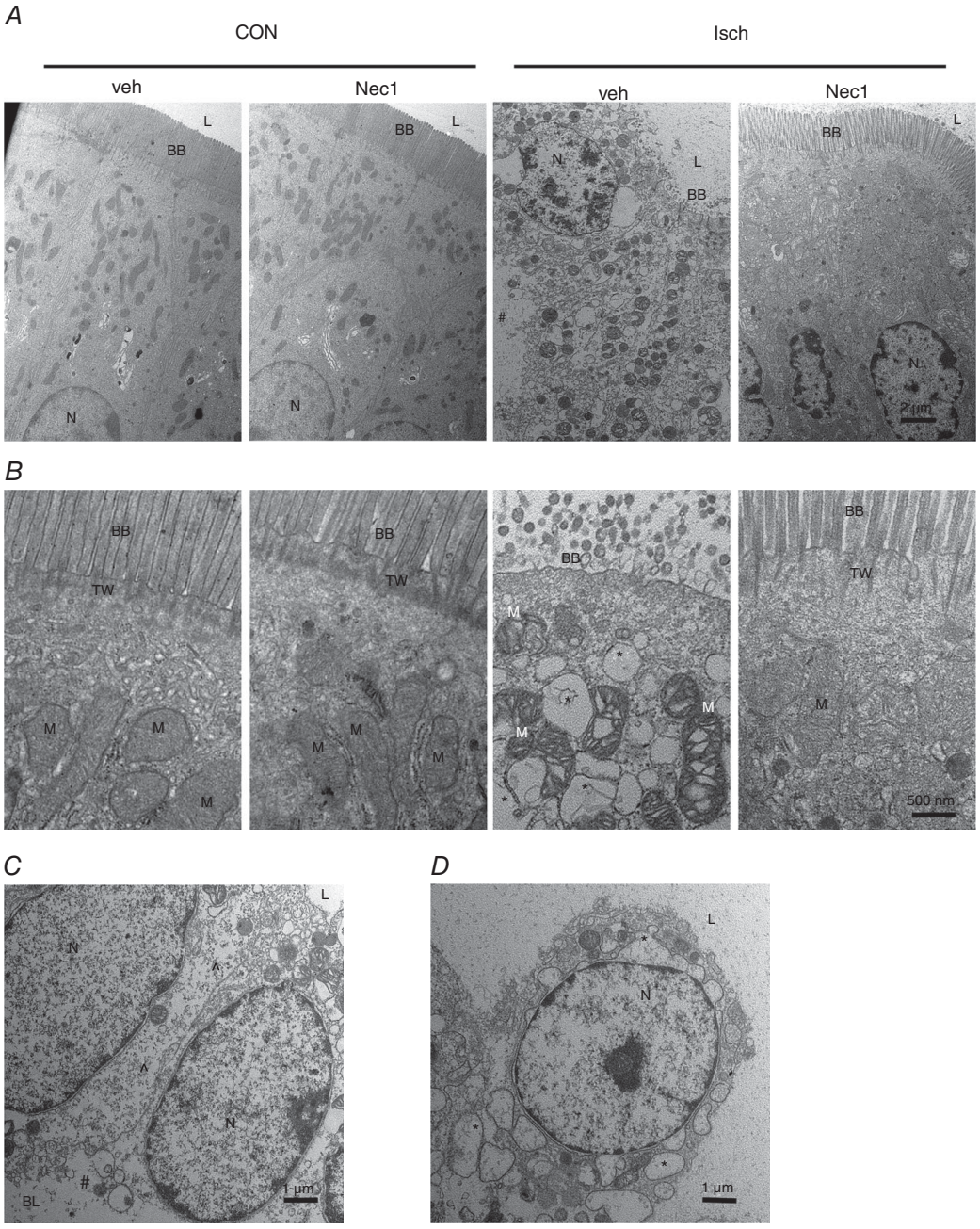

Figure 2. Ultrastructural damage in intestinal epithelial cells was observed following mesenteric ischaemia
Isch rats were subjected to occlusion of superior mesenteric artery for 20 min with or without Nec1, and jejunal mucosal tissues were processed for electromicroscopy. *A*, representative electromicrographs of jejunal epithelial cells in CON and Isch rats administered Nec1. Compared to normal columnar epithelial cells with lumen (L)-facing long brush border (BB) in control rats, the enterocytes in ischaemic groups exhibited abnormal morphology, including deformed microvilli and enlarged subepithelial spaces as a result of widened cell-matrix gaps (#). The cell nucleus (N) is also labelled. The epithelial morphological damage caused by ischaemia was ameliorated by Nec1. *B*, higher magnification showed orderly packed microvilli with actin cores rooted on the terminal web (TW), as well as mitochondria (M) organelles with cristae ultrastructure in control enterocytes. Aberrant microsome formation of the microvilli, loss of TW, mitochondrial swelling and cytoplasmic vacuolation (*) were noted in ischaemic groups. The ultrastructural abnormality in epithelial cells was ablated by administration of Nec1. *C*, enterocytes were dissociated from extracellular matrix in the basolateral side (BL), showing widened cell-matrix gaps (#) in ischaemic groups. Moreover, reduced density of the cytoplasm (^) was also evident in ischaemic cells. *D*, cellular fragments showing vacuoles (*) surrounding the nucleus (N) and an absence of subcellular organelles as a result of the loss of plasma membrane in ischaemic groups.

necroptosis in the epithelium, and also improved the villus necrotic features and mucosal histopathological scores (Fig. 3*B*–*D*). However, unlike glucose, pyruvate did not increase the mucosal ATP levels during ischaemia, suggesting that pyruvate-mediated death resistance may be exerted through an energy-independent process (Fig. 3*E*).

Next, the role of pyruvate in glucose protection against crypt dysfunction was examined. Ischaemic tissues displayed decreased levels of epithelial proliferation as indicated by a reduction in PCNA and Ki67 immunoreactivity in the crypt regions (Fig. 4*A* and *B*). Enteral instillation of glucose increased crypt PCNA and Ki67 staining in ischaemic intestines, whereas pyruvate instillation did not (Fig. 4*A* and *B*). Quantification results showed that ischaemia caused a reduction in the number of Ki67-positive cells per crypt, and this phenomenon

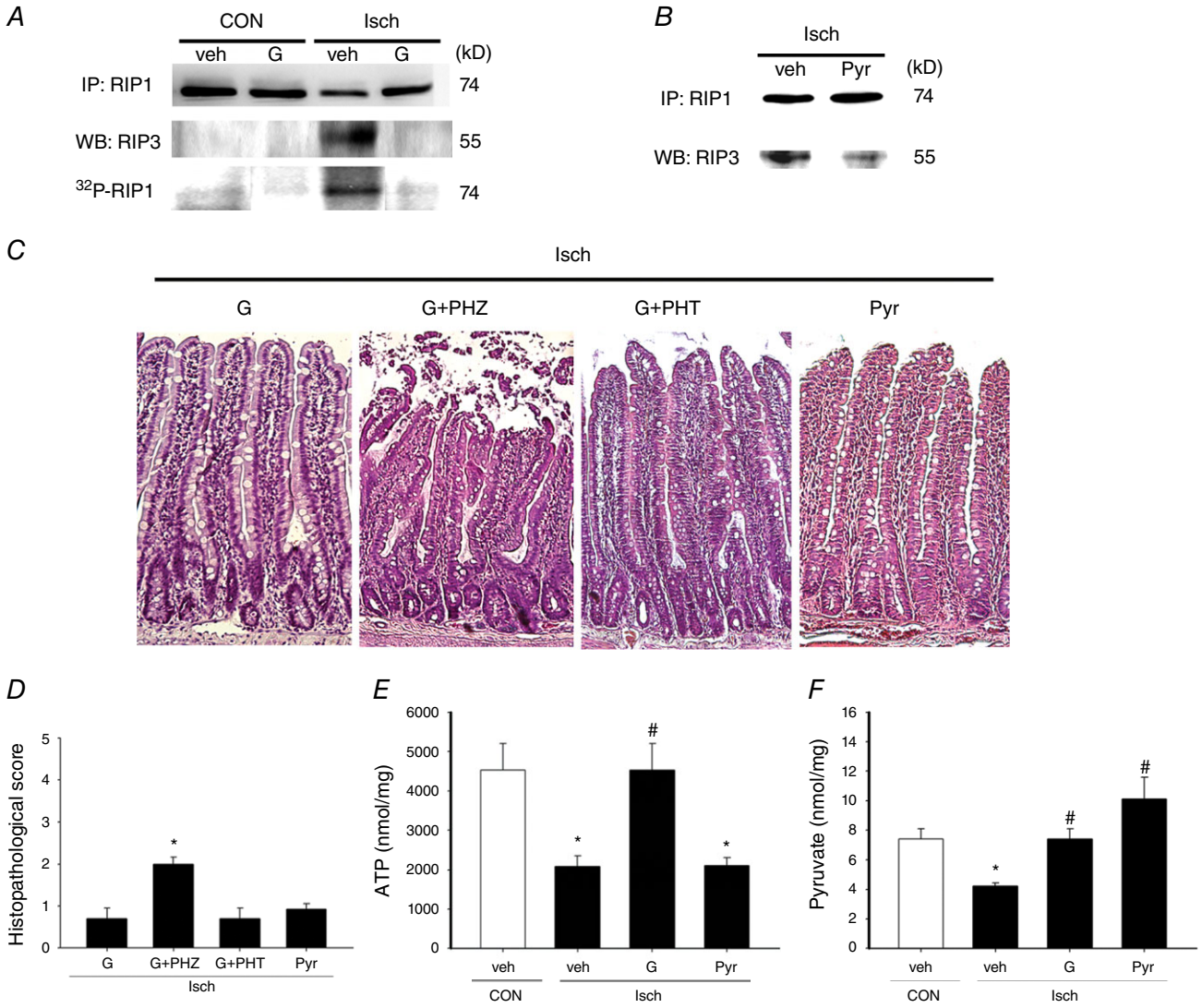

Figure 3. Enteral instillation of glucose or pyruvate protected against RIP-dependent epithelial necroptosis in ischaemic gut
Control (CON) and Isch rats were enterally instilled with glucose (G), pyruvate (Pyr) or vehicle (veh) to examine the anti-necrotic effects. *A* and *B*, immunoprecipitation blotting showed that enteral glucose or pyruvate prevented the formation of RIP1-RIP3 complex and phosphorylation of RIP1 in the jejunal mucosa of Isch rats. The experiments were repeated twice and similar results were obtained ($n = 3$ per group). *C*, representative photoimages of the histological changes in CON and Isch rat intestines given glucose or pyruvate. Enteral glucose or pyruvate alleviated the ischaemia-induced mucosal damage and villous destruction. Administration of phloridzin (PHZ; a SGLT1 inhibitor) but not phloretin (PHT; a GLU2 inhibitor) abolished glucose protection. Magnification 200×. *D*, histopathological scores in the jejunal tissues of CON and Isch rats administered various substrates. $^{*}P < 0.05$ *vs.* 'Isch + G' ($n = 6$ per group) *E*, intracellular ATP levels in ischaemic gut tissues. *F*, pyruvate levels in gut mucosa. $^{*}P < 0.05$ *vs.* CON, $^{\#}P < 0.05$ *vs.* 'Isch + Veh' ($n = 6$ per group). [Colour figure can be viewed at wileyonlinelibrary.com]

was reversed by instillation of glucose but not pyruvate (Fig. 4*C*).

Liposomal ATP partly maintained crypt proliferation but did not inhibit epithelial necroptosis nor improve mucosal morphology

The effect of ATP on ischaemic intestine was assessed by instillation of ATP-encapsulated or empty liposomes into Isch rats. Restoration of energy levels in gut mucosa was confirmed in ischaemic intestines given liposomal ATP (Fig. 5*A*). Increased PCNA and ki67 immunoreactivity was observed in the crypt regions of ischaemic tissues after administration of liposomal ATP (Fig. 4*A* and *B*). Quantification results also showed that liposomal ATP reversed the ischaemia-induced decrease in the number of Ki67-positive cells per crypt (Fig. 4*C*). However, liposomal ATP instillation did not reduce mucosal RIP1/3 complex

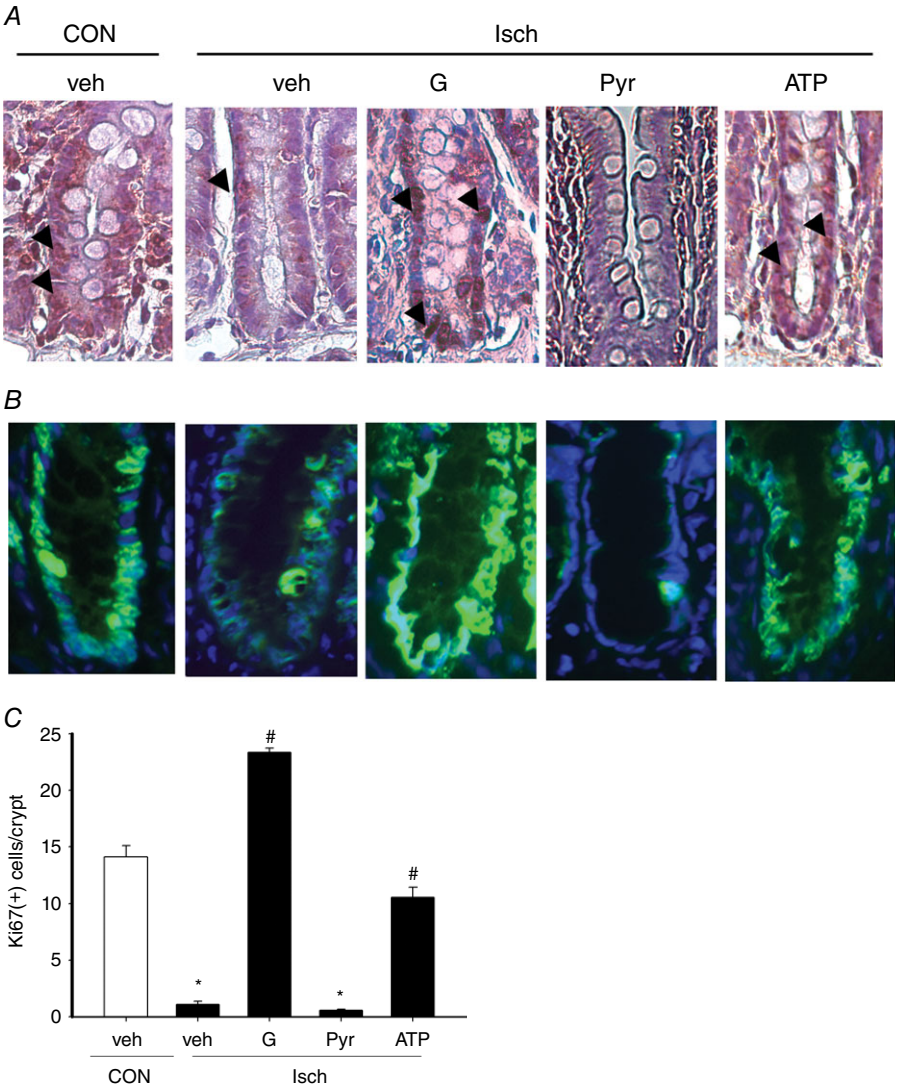

Figure 4. Ischaemia-induced loss of crypt proliferation is rescued by enteral glucose, and the glucose-mediated crypt protection is recapitulated by liposomal ATP but not by pyruvate
Isch rats were enterally instilled with glucose (G), pyruvate (Pyr), liposomal ATP (ATP) or vehicle (veh), and intestinal tissues were collected to examine crypt proliferation. *A*, immunoreactivity to PCNA (brown) in intestinal crypts. Decreased PCNA staining (arrows) was observed in intestinal crypts of Isch rats compared to control (CON) rats. Ischaemic intestines instilled with glucose and liposomal ATP but not pyruvate, showed increased PCNA staining. *B*, representative images of Ki67 staining in intestinal tissues. Reduced Ki67 immunoreactivity (green fluorescence) was detected in intestinal crypts of Isch rats compared to CON rats. Glucose and liposomal ATP but not pyruvate increased the Ki67 immunoreactivity in ischaemic tissues. The staining of Ki67 and cell nucleus (blue fluorescence) is superimposed for orientation. *C*, numbers of Ki67-positive cells per crypt in rat intestines of each group. $^{*}P < 0.05$ *vs.* CON, $^{\#}P < 0.05$ *vs.* 'Isch + Veh' ($n = 6$ per group).

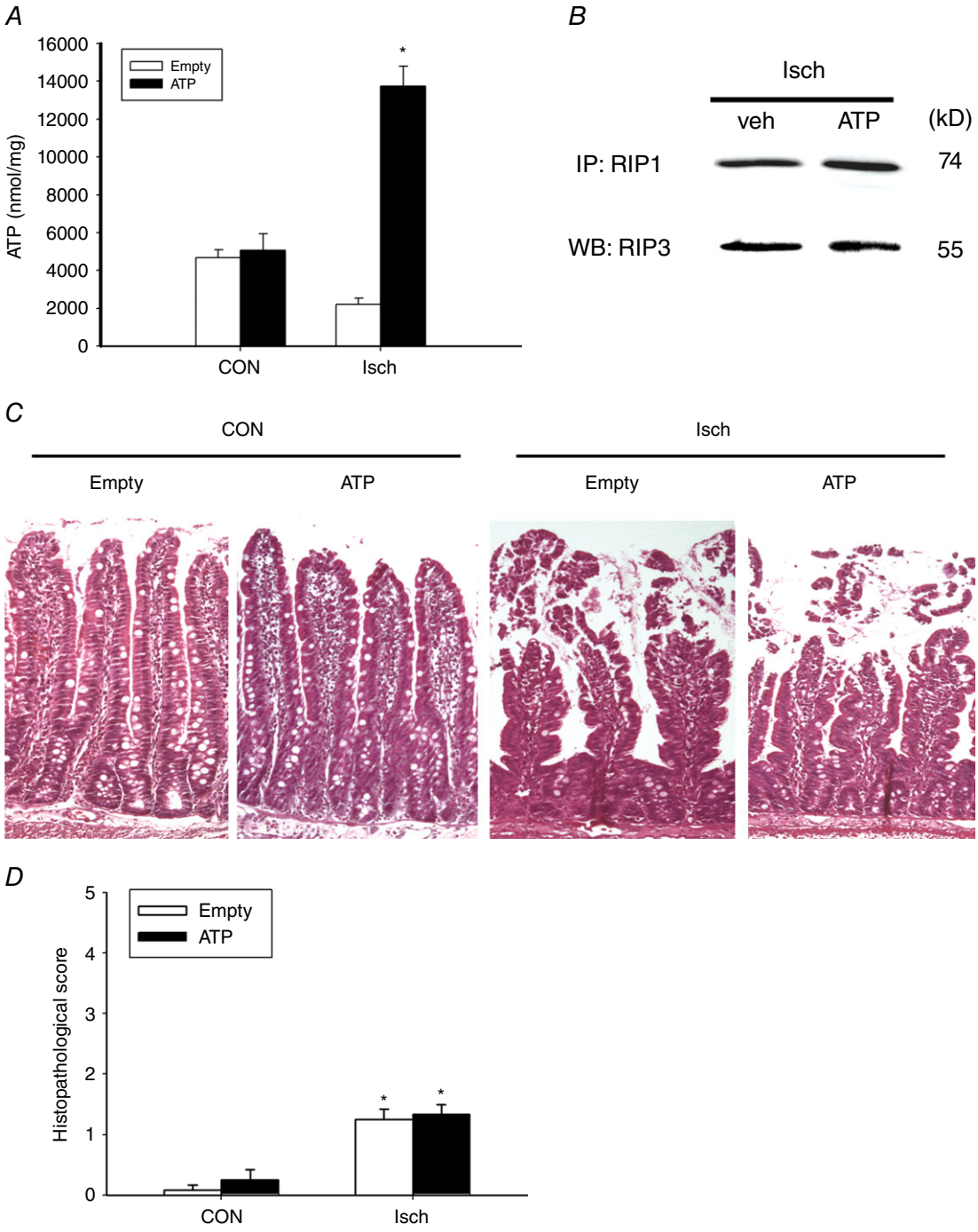

Figure 5. Restoration of ATP did not prevent epithelial necroptosis or mucosal histopathology in ischaemic gut
Isch rats were enterally administered ATP-loaded liposomes (ATP) or empty liposomes (Empty). *A*, intracellular ATP levels were measured in the gut mucosa of Isch rats. $^*P < 0.05$ *vs.* Empty ($n = 6$ per group). *B*, immunoprecipitation blotting showed the formation of RIP1-RIP3 complex in jejunal mucosa of Isch rats enterally instilled with liposomal ATP. The experiments were repeated twice and similar results were obtained ($n = 3$ per group). *C*, representative photoimages of the histological changes in CON and Isch intestines with ATP or empty liposomes. Administration of liposomal ATP did not protect against morphological damage. Magnification 200×. *D*, histopathological scores in the jejunal tissues of CON and Isch rats administered liposomal ATP or empty controls. $^*P < 0.05$ *vs.* respective CON ($n = 6$ per group). [Colour figure can be viewed at wileyonlinelibrary.com]

formation (Fig. 5*B*), nor did it improve the villus necrotic features and histopathological score in ischaemic tissues (Fig. 5*C* and *D*).

Effects of glucose, pyruvate and liposomal ATP on epithelial apoptosis caused by ischaemia

Apart from epithelial necroptosis, increased TUNEL-positive apoptotic cells were also seen in ischaemic tissues (Fig. 6). Enteral glucose and pyruvate reduced the number of apoptotic epithelial cells in ischaemic tissues to baseline control levels (Fig. 6). However, liposomal ATP only partially decreased the apoptotic levels (Fig. 6).

Reperfusion injury and bacterial translocation were also ameliorated by glucose and pyruvate but not by non-metabolizable sugars

Lastly, the protective effect of glucose and pyruvate against reperfusion-associated mucosal injury and bacterial translocation was assessed in I/R rats subjected to mesenteric ischaemia for 20 min followed by reperfusion for 60 min. Villous dismantling, epithelial abnormality with widened intercellular junctions and enlarged cell-matrix gaps were observed following I/R (Fig. 7*A* and *B*). Subcellular necrotic features were seen, including mitochondrial swelling, cytoplasmic vacuolation and cytosol density loss (Fig. 7*C*–*E*). I/R enterocytes also displayed numerous apical regions denuded of microvilli; the microvilli that remained present were in the form of microsomes or sequential banding (Fig. 7*D* and *E*). Moreover, epithelial repair showing a flattened epithelium at the edge of denuded area as evidence of restitution during reperfusion was also seen in I/R rats (Fig. 7*A*). The I/R-induced necrotic features and histopathology were abolished by enteral instillation of glucose or pyruvate (Fig. 7*A* and *F*) but not by non-metabolizable sugars (i.e. 3-OMG, mannitol) or amino acid (i.e. glutamate) (Fig. 7*F* and *G*).

Intestinal permeability changes were evaluated by lumen-to-blood passage of fluorescein-conjugated dextran (molecular weight = 30,00) or monitored by portal influx of a contrast agent Gd (molecular weight = 574) using real-time MRI. I/R-increased intestinal permeability was reduced by enteral instillation of glucose or pyruvate but not by other non-metabolizable substances (Fig. 8*A* and *B*). Lastly, bacterial translocation to extraintestinal organs was used as an indicator of gut-derived sepsis. The bacterial counts in the liver and spleen tissues were significantly decreased by glucose and pyruvate (Fig. 8*C*).

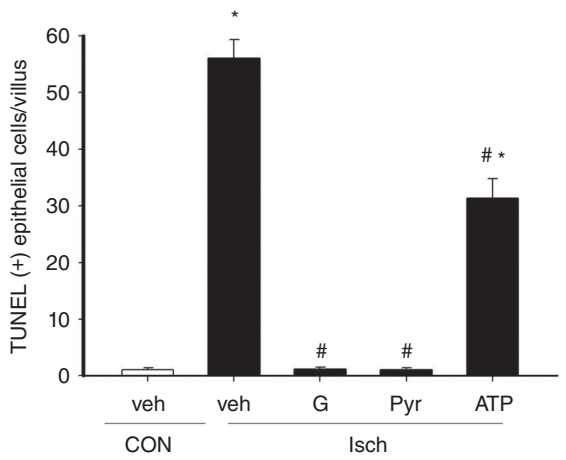

Figure 6. Enteral instillation of glucose or pyruvate protected against epithelial apoptosis in an energy-independent manner in ischaemic gut
Rats were subjected to sham operation as controls (CON) or mesenteric ischaemia (Isch). Isch rats were enterally instilled vehicle (veh), glucose (G), pyruvate (Pyr) or liposomal ATP (ATP) and epithelial apoptosis in intestinal tissues was measured using a TUNEL assay. The number of TUNEL-positive epithelial cells per villus was determined. $^{*}P < 0.05$ *vs.* respective CON, $^{\#}P < 0.05$ *vs.* 'Isch + Veh' ($n = 6$ per group).

Discussion

The present study provides evidence of a novel form of necrotic death in ischaemic enterocytes that involves the assembly and phosphorylation of RIP1/3 complex. The ischaemia-induced epithelial cell death, loss of crypt proliferation and mucosal morphological damage are protected by enteral glucose uptake. Our data indicate that glucose metabolites (i.e. pyruvate and ATP) play distinct cytoprotective roles in ischaemic gut. Administration of pyruvate inhibited epithelial necroptotic death but did not rescue against crypt dysfunction, whereas replenishment of ATP partly restored crypt proliferation but failed to rescue cell necroptosis.

Abundant studies showed epithelial cell death (both apoptosis and necrosis) with widened cell-cell and cell-matrix gaps following I/R challenge, resulting in intestinal barrier dysfunction and bacterial translocation (Shah *et al.* 1997; Little *et al.* 2003; Azuara *et al.* 2005; Huang *et al.* 2011). Glucose instillation is well known for being protective against mucosal morphological and barrier damage caused by ischaemic insults; however, the detailed mechanisms responsible for this remain unclear (Kozar *et al.* 2002; Huang *et al.* 2011). Anaerobic glycolytic pathway converts one glucose molecule to two pyruvates, which also generates two ATP through the process catalysed by pyruvate kinase. Pyruvate then feeds into the tricarboxylic acid cycle in mitochondrial respiration for oxygen-dependent ATP production (Huang & Yu, 2015). In the present study, we assessed the protective effects of distinct glucose metabolites (pyruvate and ATP) on two aspects of ischaemia-induced epithelial injury, including cell death and crypt dysfunction.

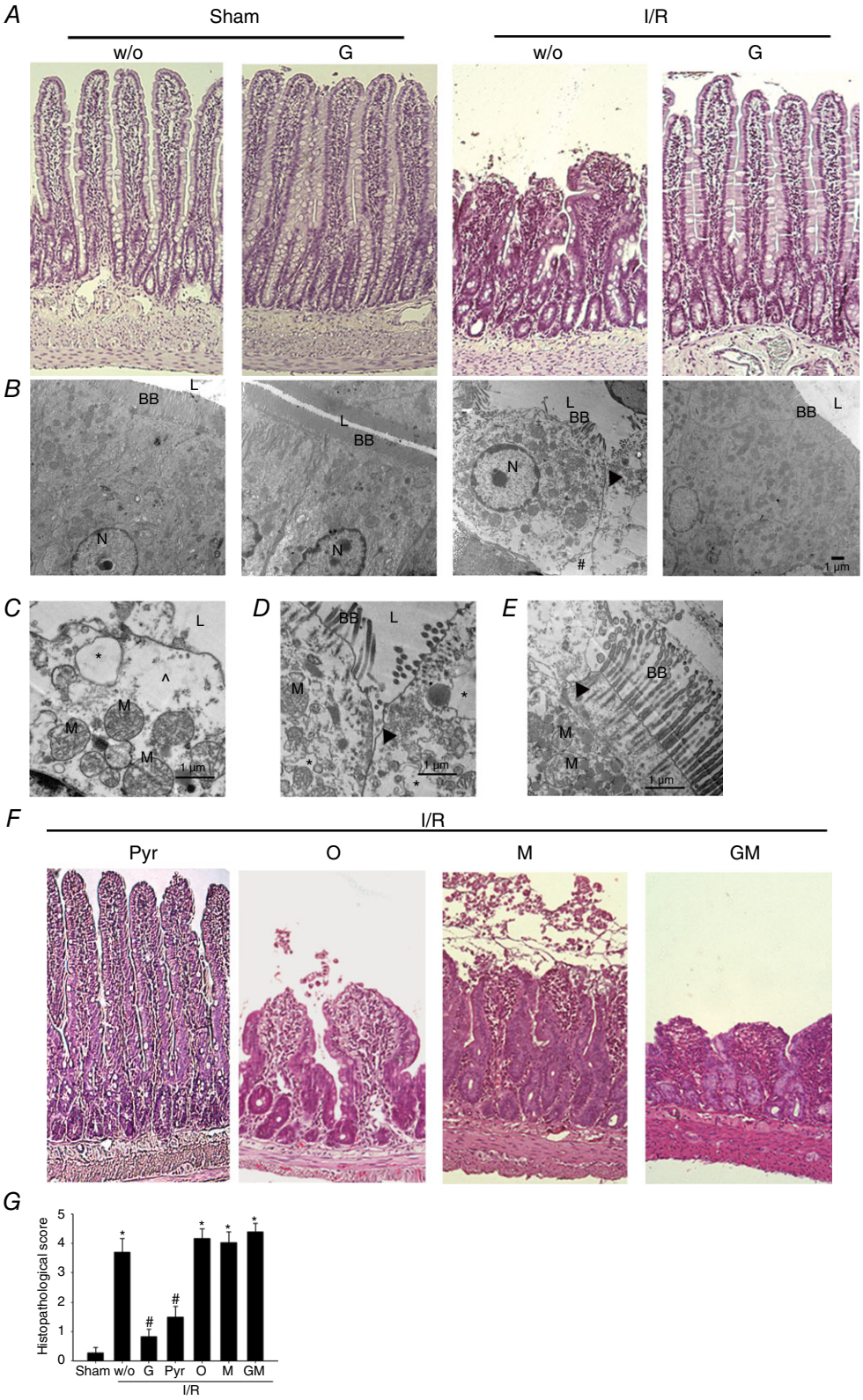

Figure 7. Reperfusion-associated villous histopathology and epithelial necrosis were ameliorated by enteral instillation of glucose and pyruvate but not 3-OMG, mannitol or glutamate
Rats were subjected to sham-operation (Sham) and I/R with or without enteral instillation of glucose (G) and pyruvate (Pyr) and the jejunal tissues were processed for haematoxylin and eosin staining and transmission electron microscopy imaging. *A*, villous blunting and dismantling in intestines of I/R rats were alleviated by enteral instillation

Our previous studies demonstrated that glucose uptake prevented caspase-dependent apoptosis in enterocytes after mesenteric I/R (Huang *et al.* 2011). The data in the present study show that pyruvate attenuated the RIP1/3-dependent necroptosis in epithelial cells after ischaemic insults, whereas replenishment of ATP failed to modulate necroptotic epithelial death. On the other hand, the maintenence of crypt proliferation in ischaemic gut by glucose was recapitulated by the administration of liposomal ATP but not of pyruvate, suggesting that glucose metabolism and ATP synthesis restored crypt function. Although pyruvate is the starting substance in the tricarboxylate cycle, pyruvate instillation during ischaemia may not lead to ATP generation by mitochondrial respiration as a result of the low oxygen levels. Indeed, instillation of glucose during ischaemia increase tissue ATP levels but pyruvate did not. In addition to glucose metabolism, SGLT1-mediated signalling pathways such as PI3K/Akt and NF-κB (Palazzo *et al.* 2008; Huang *et al.* 2011) may also be involved in glucose-promoted epithelial renewal and proliferation. The present study is the first to tease out the specific site and modes of action for glucose metabolites to exert cytoprotection in ischaemic intestine.

Numerous studies, including those in intestine and sterile organs, have attributed glucose-mediated cytoprotection against ischaemic injury to its ability for energy replenishment (Inci *et al.* 2001; Fu *et al.* 2014; Wei *et al.* 2014; Qi & Young, 2015). However, unlike others showing beneficial effects of liposomal ATP to ischaemic injury in neurons, myocardiocytes and the retina (Dvoriantchikova *et al.* 2010; Levchenko *et al.* 2010; Liu *et al.* 2013), we did not see a reduction in histopathological score in intestinal ischaemia, despite partial restoration of crypt proliferation following ATP administration. This discrepancy may be a result of the severe epithelial cell death (which was not protected by ATP) leading to massive bacterial influx accompanied by inflammation and secondary tissue injury. Thus, ATP-promoting crypt proliferation was insufficient to alter the course of ischaemic injury.

In the present study, ATP-encapsulated liposomes were utilized for the direct delivery of ATP into epithelial cells in comparison to enteral nutrient-derived energy metabolism. Amino acids such as glutamine and glutamate are metabolic energy fuels that utilize the mitochondrial oxidative pathways of tricarboxylic acid cycle for ATP synthesis (Fleming *et al.* 1997; Reeds *et al.* 2000). The use of liposomal ATP delivery instead of metabolic energy fuels aimed to ensure that cells acquire ATP even if mitochondrial oxidative phosphorylation was shut down during ischaemic/hypoxic conditions. Compared to pyruvate, glutamate did not reduce mucosal histopathology, epithelial permeability or bacterial translocation in I/R rats in the present study. Glutamate serves as a valuable control for glycolytic pyruvate because both enter the mitochondrial tricarboxylic acid cycle under normoxic conditions. We suspect that, in the ischaemic/hypoxic condition, both substrates did not undergo mitochondria-dependent oxidative energy metabolism, further indicating that epithelial death resistance by pyruvate was uncoupled from ATP production. Furthermore, abundant studies have shown that glutamine protects against epithelial barrier function and bacterial translocation in rodent and porcine models of intestinal I/R (Blikslager *et al.* 1999; Kozar *et al.* 2002; Kozar *et al.* 2004*a*; Sato *et al.* 2005; Medeiros *et al.* 2006). Unpublished data obtained in our laboratory also show that enteral instillation of glutamine reduced epithelial barrier dysfunction in I/R rats (CY Huang and LCH Yu, unpublished data). However, the protective effects of glutamine have been attributed to two factors, which include serving as an oxidative metabolic fuel and acting as an immune-enhancing agent (Kozar *et al.* 2004*b*; Sato *et al.* 2005). Therefore, we did not conduct further experiments to study the effect of glutamine on epithelial necroptosis because of its immunomodulatory role, which might confound data interpretation.

Our previous study indicated that pyruvate scavenges mitochondrial free radicals and inhibits necroptosis in hypoxic cells (Huang *et al.* 2013). In the present study, we showed that pyruvate inhibited epithelial necroptosis during ischaemia, and also prevented epithelial permeability increase and bacterial translocation after

of glucose. Magnification 200×. *B*, representative electromicrographs showing I/R-induced ultrastructural damage in epithelial cells may be prevented by glucose. Compared to the tightly linked columnar cells with lumen (L)-facing long brush border (BB) in sham controls, I/R enterocytes exhibited round-shape morphology with effacing microvilli, widened intercellular junctions (arrowhead) and enlarged cell-matrix gaps (#). The I/R-induced epithelial damage was ameliorated by glucose instillation. The cell nucleus (N) was also labelled in images. *C*, higher magnification of I/R enterocytes showing subcellular abnormalities, including mitochondrial (M) swelling, cytoplasmic vacuolation (*) and cytosol density loss (^). *D* and *E*, higher magnification of I/R enterocytes displayed widened intercellular junctions (arrowhead) and numerous apical regions denuded of microvilli, and those that remain present are in the form of sequential constrictions, and often appeared to be disintegrating into microsomes. *F*, replacement of glucose with pyruvate (Pyr) also protected mucosal injury. However, replacement by 3-OMG (O), mannitol (M) or glutamate (GM) did not ameliorate the morphological damage in I/R intestines. Magnification 200×. *G*, histopathological scores in jejunal tissues of Sham and I/R rats with enteral instillation of glucose, pyruvate, 3-OMG, mannitol and glutamate. $^{*}P < 0.05$ *vs.* sham, $^{\#}P < 0.05$ *vs.* 'I/R + w/o' ($n = 6$–8 per group). [Colour figure can be viewed at wileyonlinelibrary.com]

blood reperfusion. The results are in keeping with early reports demonstrating that I.V. and intraluminal administration of ethyl pyruvate or sodium pyruvate attenuated reperfusion-induced oxidative free radical levels and prevented mucosal barrier dysfunction (Cicalese *et al.* 1996; Sims *et al.* 2001; Cruz *et al.* 2011; Petrat *et al.* 2011). Together with our studies, these findings suggest that the anti-oxidant characteristics of glycolytic pyruvate

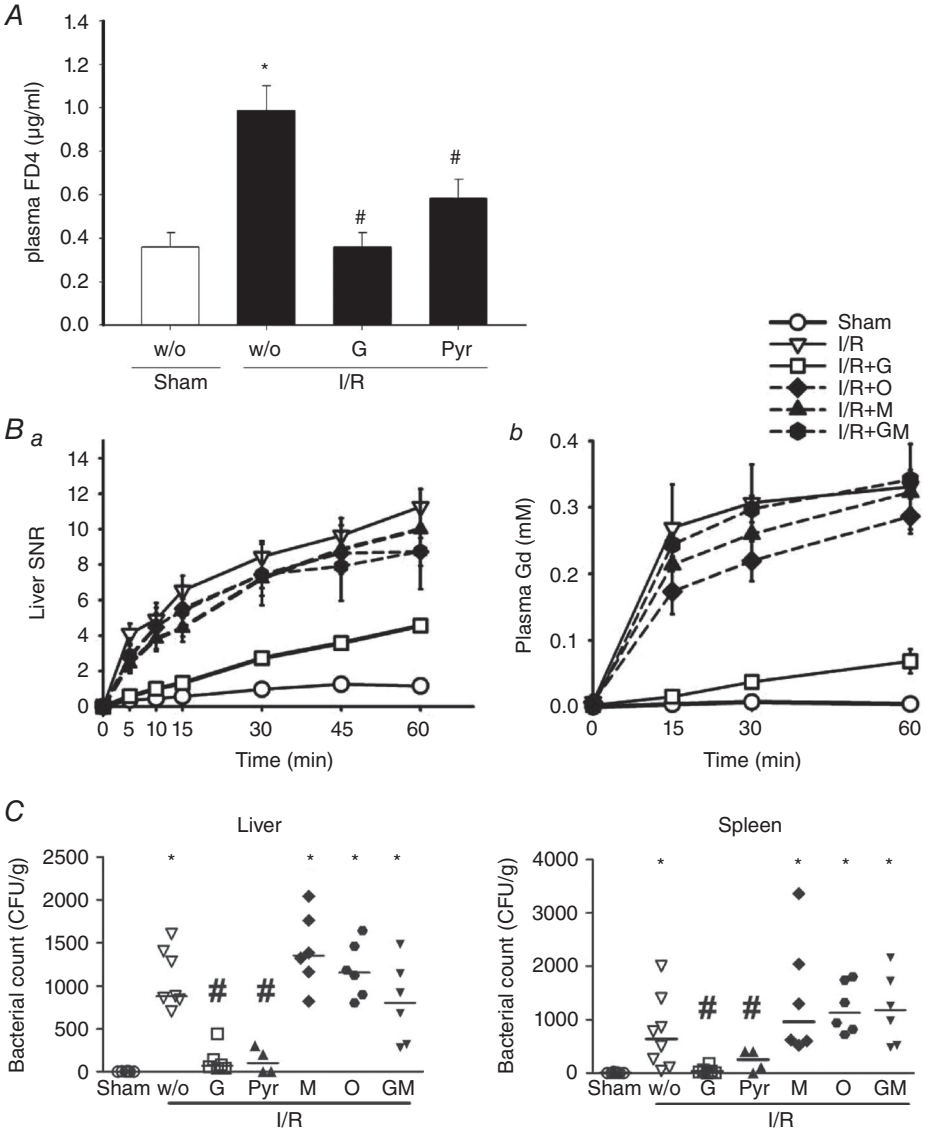

Figure 8. Intestinal I/R-induced epithelial permeability rise was diminished by enteral instillation of glucose and pyruvate

The intestinal permeability of sham-operated (Sham) and ischaemia/reperfusion (I/R) rats with or without enteral instillation of glucose (G) and pyruvate (Pyr) was assessed. *A*, 4-kDa FITC-dextran (FD4) concentration in plasma sample collected from sham, I/R + w/o, I/R + G and I/R + Pyr rats at 60 min post-reperfusion. A significant increase of lumen-to-blood passage of FD4 was seen in I/R rats compared to sham controls, which was decreased by instillation of glucose and pyruvate. *B*, increased the signal-to-noise ratio (SNR) of Gd in the liver (*Ba*) and the Gd concentration in plasma samples (*Bb*) was found in I/R rats compared to Sham rats, suggesting enhanced portal drainage of enterally administered Gd after reperfusion. Enteral instillation of glucose but not 3-OMG mannitol or glutamate reduced the increase of liver, kidney and plasma signals. Statistical labels were omitted for clarity ($n = 6$ per group). *C*, bacterial counts in liver and spleen were determined in Sham and I/R rats. Each data point represents the bacterial CFU from one animal, and the median values are shown as bars. The increase in liver and spleen bacterial counts in I/R rats was reduced by enteral instillation of glucose and pyruvate but not other substances (i.e. 3-OMG, mannitol or glutamate). $^{*}P < 0.05$ *vs.* sham; $^{\#}P < 0.05$ *vs.* 'I/R + w/o' ($n = 6$–8 per group).

may underlie the mechanisms of its protection against ischaemia- and reperfusion-induced epithelial cell death.

Although concerns were raised regarding whether glucose uptake and glycolytic ATP may cause a switch from necrosis to apoptosis, as previously shown in ischaemic hepatocytes (Kim *et al.* 2003), our previous and current data show a decrease in apoptotic levels after glucose and pyruvate instillation in ischaemic gut (Huang *et al.* 2011). In addition, glucose and pyruvate attenuated necroptosis and apoptotic death in an ATP-independent manner. Taken together, it is plausible that glucose and pyruvate (uncoupled from ATP) are capable of preventing ischaemic cells from undergoing either class of programmed cell death, rather than inducing a mode switch.

Upon facing metabolic and oxidative crisis (e.g. hypoxia and nutrient deprivation), different modes and orders of cell death including apoptosis, necroptosis or necrosis, may occur (Huang & Yu, 2015). In the present study, prolonged ischaemia after 60—120 min resulted in RIP-independent epithelial necrosis, which could not be protected by enteral instillation of glucose or pyruvate (data not shown). It remains unclear whether cell death modes occur in a sequential or overlapping order, and controversial data exist regarding the critical trigger(s) responsible for each death mode or for mode switching (i.e. sensing of oxygen drop, energy depletion or acidity increase) (Taylor, 2008; Chandel, 2010; Holzer, 2011). Our study challenges the notion that energy depletion is the initiating factor for triggering cell death under ischaemic stress. Overall, glycolytic pyruvate uncoupled from energy synthesis played a protective role against various modes of programmed cell death (i.e. apoptosis and necroptosis).

In conclusion, glucose metabolites play distinct cytoprotective roles in intestinal ischaemia. Pyruvate attenuated epithelial necroptosis and apoptosis in an ATP-independent manner, whereas energy replenishment partially restored crypt proliferation but did not prevent cell death in ischaemic gut. Our data argue against the traditional view of ATP as the main cytoprotective factor by enteral glucose metabolism, and indicate a novel anti-necroptotic role of glycolytic pyruvate under ischaemic stress.

References

Azuara D, Sola A, Hotter G, Calatayud L & de Oca J (2005). Apoptosis inhibition plays a greater role than necrosis inhibition in decreasing bacterial translocation in experimental intestinal transplantation. *Surgery* **137**, 85–91.

Blikslager AT, Rhoads JM, Bristol DG, Roberts MC & Argenzio RA (1999). Glutamine and transforming growth factor-alpha stimulate extracellular regulated kinases and enhance recovery of villous surface area in porcine ischemic-injured intestine. *Surgery* **125**, 186–194.

Chakrabarti G, Zhou X & McClane BA (2003). Death pathways activated in CaCo-2 cells by *Clostridium perfringens* enterotoxin. *Infect Immun* **71**, 4260–4270.

Chandel NS (2010). Mitochondrial regulation of oxygen sensing. *Adv Exp Med Biol* **661**, 339–354.

Chen TL, Chen S, Wu HW, Lee TC, Lu YZ, Wu LL, Ni YH, Sun CH, Yu WH, Buret AG & Yu LC (2013). Persistent gut barrier damage and commensal bacterial influx following eradication of *Giardia* infection in mice. *Gut Pathog* **5**, 26.

Cheng CH, Lin HC, Lai IR & Lai HS (2013). Ischemic postconditioning attenuate reperfusion injury of small intestine: impact of mitochondrial permeability transition. *Transplantation* **95**, 559–565.

Cho YS, Challa S, Moquin D, Genga R, Ray TD, Guildford M & Chan FK (2009). Phosphorylation-driven assembly of the RIP1-RIP3 complex regulates programmed necrosis and virus-induced inflammation. *Cell* **137**, 1112–1123.

Cicalese L, Lee K, Schraut W, Watkins S, Borle A & Stanko R (1996). Pyruvate prevents ischemia-reperfusion mucosal injury of rat small intestine. *Am J Surg* **171**, 97–100.

Cruz RJ, Jr., Harada T, Sasatomi E & Fink MP (2011). Effects of ethyl pyruvate and other alpha-keto carboxylic acid derivatives in a rat model of multivisceral ischemia and reperfusion. *J Surg Res* **165**, 151–157.

Debus ES, Muller-Hulsbeck S, Kolbel T & Larena-Avellaneda A (2011). Intestinal ischemia. *Int J Colourectal Dis* **26**, 1087–1097.

Declercq W, Vanden Berghe T & Vandenabeele P (2009). RIP kinases at the crossroads of cell death and survival. *Cell* **138**, 229–232.

Dvoriantchikova G, Barakat DJ, Hernandez E, Shestopalov VI & Ivanov D (2010). Liposome-delivered ATP effectively protects the retina against ischemia-reperfusion injury. *Mol Vis* **16**, 2882–2890.

Eltzschig HK, Bratton DL & Colgan SP (2014). Targeting hypoxia signalling for the treatment of ischaemic and inflammatory diseases. *Nat Rev Drug Discov* **13**, 852–869.

Fink MP (2010). The therapeutic potential of pyruvate. *J Surg Res* **164**, 218–220.

Fleming SE, Zambell KL & Fitch MD (1997). Glucose and glutamine provide similar proportions of energy to mucosal cells of rat small intestine. *Am J Physiol Gastrointestinal Liver Physiology* **273**, G968–G978.

Fu H, Xu H, Chen H, Li Y, Li W, Zhu Q, Zhang Q, Yuan H, Liu F, Wang Q, Miao M & Shi X (2014). Inhibition of glycogen synthase kinase 3 ameliorates liver ischemia/reperfusion injury via an energy-dependent mitochondrial mechanism. *J Hepatol* **61**, 816–824.

Gunther C, Martini E, Wittkopf N, Amann K, Weigmann B, Neumann H, Waldner MJ, Hedrick SM, Tenzer S, Neurath MF & Becker C (2011). Caspase-8 regulates TNF-alpha-induced epithelial necroptosis and terminal ileitis. *Nature* **477**, 335–339.

He S, Wang L, Miao L, Wang T, Du F, Zhao L & Wang X (2009). Receptor interacting protein kinase-3 determines cellular necrotic response to TNF-alpha. *Cell* **137**, 1100–1111.

Holzer P (2011). Acid sensing by visceral afferent neurones. *Acta Physiol (Oxf)* **201**, 63–75.

Hsiao JK, Huang CY, Lu YZ, Yang CY & Yu LCH (2009). Magnetic resonance imaging detects intestinal barrier dysfunction in a rat model of acute mesenteric ischemia/reperfusion injury. *Invest Radiol* **44**, 329–335.

Huang CY, Hsiao JK, Lu YZ, Lee CT & Yu LCH (2011). Anti-apoptotic PI3K/Akt signalling by sodium/glucose transporter 1 reduces epithelial barrier damage and bacterial translocation in intestinal ischemia. *Lab Invest* **91** 294–309.

Huang CY, Kuo WT, Huang YC, Lee TC & Yu LC (2013). Resistance to hypoxia-induced necroptosis is conferred by glycolytic pyruvate scavenging of mitochondrial superoxide in colourectal cancer cells. *Cell Death Dis* **4**, e622.

Huang CY & Yu LC (2015). Pathophysiological mechanisms of death resistance in colourectal carcinoma. *World J Gastroenterol* **21** 11777–11792.

Inci I, Dutly A, Rousson V, Boehler A & Weder W (2001). Trimetazidine protects the energy status after ischemia and reduces reperfusion injury in a rat single lung transplant model. *J Thorac Cardiovasc Surg* **122**, 1155–1161.

Kalischuk LD, Inglis GD & Buret AG (2007). Strain-dependent induction of epithelial cell oncosis by *Campylobacter jejuni* is correlated with invasion ability and is independent of cytolethal distending toxin. *Microbiology* **153**, 2952–2963.

Kao KK & Fink MP (2010). The biochemical basis for the anti-inflammatory and cytoprotective actions of ethyl pyruvate and related compounds. *Biochem Pharmacol* **80**, 151–159.

Kim JS, He L, Qian T & Lemasters JJ (2003). Role of the mitochondrial permeability transition in apoptotic and necrotic death after ischemia/reperfusion injury to hepatocytes. *Curr Mol Med* **3**, 527–535.

Kozar RA, Schultz SG, Bick RJ, Poindexter BJ, DeSoignie R & Moore FA (2004*a*). Enteral glutamine but not alanine maintains small bowel barrier function after ischemia/reperfusion injury in rats. *Shock* **21**, 433–437.

Kozar RA, Schultz SG, Hassoun HT, DeSoignie R, Weisbrodt NW, Haber MM & Moore FA (2002). The type of sodium-coupled solute modulates small bowel mucosal injury, transport function, and ATP after ischemia/reperfusion injury in rats. *Gastroenterology* **123**, 810–816.

Kozar RA, Verner-Cole E, Schultz SG, Sato N, Bick RJ, DeSoignie R, Poindexter BJ & Moore FA (2004*b*). The immune-enhancing enteral agents arginine and glutamine differentially modulate gut barrier function following mesenteric ischemia/reperfusion. *J Trauma* **57**, 1150–1156.

Kuo WT, Lee TC, Yang HY, Chen CY, Au YC, Lu YZ, Wu LL, Wei SC, Ni YH, Lin BR, Chen Y, Tsai YH, Kung JT, Sheu F, Lin LW & Yu LC (2015). LPS receptor subunits have antagonistic roles in epithelial apoptosis and colonic carcinogenesis. *Cell Death Differ* **22**, 1590–1604.

Levchenko TS, Hartner WC, Verma DD, Bernstein EA & Torchilin VP (2010). ATP-loaded liposomes for targeted treatment in models of myocardial ischemia. *Meth Mol Biol* **605**, 361–375.

Liang X, Chen Y, Zhang L, Jiang F, Wang W, Ye Z, Liu S, Yu C & Shi W (2014). Necroptosis, a novel form of caspase-independent cell death, contributes to renal epithelial cell damage in an ATP-depleted renal ischemia model. *Mol Med Rep* **10**, 719–724.

Little D, Dean RA, Young KM, McKane SA, Martin LD, Jones SL & Blikslager AT (2003). PI3K signalling is required for prostaglandin-induced mucosal recovery in ischemia-injured porcine ileum. *Am J Physiol Gastrointest Liver Physiol* **284**, G46–G56.

Liu S, Zhen G, Li RC & Dore S (2013). Acute bioenergetic intervention or pharmacological preconditioning protects neuron against ischemic injury. *J Exp Stroke & Transl Med* **6**, 7–17.

Lu YZ, Wu CC, Huang YC, Huang CY, Yang CY, Lee TC, Chen CF & Yu LC (2012). Neutrophil priming by hypoxic preconditioning protects against epithelial barrier damage and enteric bacterial translocation in intestinal ischemia/reperfusion. *Lab Invest* **92**, 783–796.

Luedde M, Lutz M, Carter N, Sosna J, Jacoby C, Vucur M, Gautheron J, Roderburg C, Borg N, Reisinger F, Hippe HJ, Linkermann A, Wolf MJ, Rose-John S, Lullmann-Rauch R, Adam D, Flogel U, Heikenwalder M, Luedde T & Frey N (2014). RIP3, a kinase promoting necroptotic cell death, mediates adverse remodelling after myocardial infarction. *Cardiovasc Res* **103**, 206–216.

Medeiros AC, Chacon DA, Sales VS, Egito ES, Brandao-Neto J, Pinheiro LA & Carvalho MR (2006). Glucan and glutamine reduce bacterial translocation in rats subjected to intestinal ischemia-reperfusion. *J Invest Surg* **19**, 39–46.

Palazzo M, Gariboldi S, Zanobbio L, Selleri S, Dusio GF, Mauro V, Rossini A, Balsari A & Rumio C (2008). Sodium-dependent glucose transporter-1 as a novel immunological player in the intestinal mucosa. *J Immunol* **181**, 3126–3136.

Peng PC, Hong RL, Tsai YJ, Li PT, Tsai T & Chen CT (2015). Dual-effect liposomes encapsulated with doxorubicin and chlorin e6 augment the therapeutic effect of tumor treatment. *Lasers Surg Med* **47**, 77–87.

Petrat F, Ronn T & de Groot H (2011). Protection by pyruvate infusion in a rat model of severe intestinal ischemia-reperfusion injury. *J Surg Res* **167**, e93–e101.

Pierdomenico M, Negroni A, Stronati L, Vitali R, Prete E, Bertin J, Gough PJ, Aloi M & Cucchiara S (2014). Necroptosis is active in children with inflammatory bowel disease and contributes to heighten intestinal inflammation. *Am J Gastroenterol* **109**, 279–287.

Qi D & Young LH (2015). AMPK: energy sensor and survival mechanism in the ischemic heart. *Trends Endocrinol Metab* **26**, 422–429.

Reeds PJ, Burrin DG, Stoll B & Jahoor F (2000). Intestinal glutamate metabolism. *J Nutr* **130**, 978S–982S.

Sato N, Moore FA, Smith MA, Zou L, Moore-Olufemi S, Schultz SG & Kozar RA (2005). Immune-enhancing enteral nutrients differentially modulate the early proinflammatory transcription factors mediating gut ischemia/reperfusion. *J Trauma* **58**, 455–461.

Scheepers A, Joost HG & Schurmann A (2004). The glucose transporter families SGLT and GLUT: molecular basis of normal and aberrant function. *JPEN J Parent Ent Nutr* **28**, 364–371.

Schulz S, Wong RJ, Jang KY, Kalish F, Chisholm KM, Zhao H, Vreman HJ, Sylvester KG & Stevenson DK (2013). Heme oxygenase-1 deficiency promotes the development of necrotizing enterocolitis-like intestinal injury in a newborn mouse model. *Am J Physiol Gastrointest Liver Physiol* **304**, G991–G1001.

Shah KA, Shurey S & Green CJ (1997). Apoptosis after intestinal ischemia-reperfusion injury: a morphological study. *Transplantation* **64**, 1393–1397.

Sims CA, Wattanasirichaigoon S, Menconi MJ, Ajami AM & Fink MP (2001). Ringer's ethyl pyruvate solution ameliorates ischemia/reperfusion-induced intestinal mucosal injury in rats. *Crit Care Med* **29**, 1513–1518.

Taylor CT (2008). Mitochondria and cellular oxygen sensing in the HIF pathway. *Biochem J* **409**, 19–26.

Temkin V, Huang Q, Liu H, Osada H & Pope RM (2006). Inhibition of ADP/ATP exchange in receptor-interacting protein-mediated necrosis. *Mol Cell Biol* **26**, 2215–2225.

Vanlangenakker N, Vanden Berghe T, Krysko DV, Festjens N & Vandenabeele P (2008). Molecular mechanisms and pathophysiology of necrotic cell death. *Curr Mol Med* **8**, 207–220.

Wei Q, Xiao X, Fogle P & Dong Z (2014). Changes in metabolic profiles during acute kidney injury and recovery following ischemia/reperfusion. *PLoS One* **9**, e106647.

Welz PS, Wullaert A, Vlantis K, Kondylis V, Fernandez-Majada V, Ermolaeva M, Kirsch P, Sterner-Kock A, van Loo G & Pasparakis M (2011). FADD prevents RIP3-mediated epithelial cell necrosis and chronic intestinal inflammation. *Nature* **477**, 330–334.

Wu LL, Chiu HD, Peng WH, Lin BR, Lu KS, Lu YZ & Yu LCH (2011). Epithelial inducible nitric oxide synthase causes bacterial translocation by impairment of enterocytic tight junctions via intracellular signals of Rho-associated kinase and protein kinase C zeta. *Crit Care Med* **39**, 2087–2098.

Wu LL, Peng WH, Kuo WT, Huang CY, Ni YH, Lu KS, Turner JR & Yu LC (2014). Commensal bacterial endocytosis in epithelial cells is dependent on myosin light chain kinase-activated brush border fanning by interferon-gamma. *Am J Pathol* **184**, 2260–2274.

Yin B, Xu Y, Wei RL, He F, Luo BY & Wang JY (2015). Inhibition of receptor-interacting protein 3 upregulation and nuclear translocation involved in necrostatin-1 protection against hippocampal neuronal programmed necrosis induced by ischemia/reperfusion injury. *Brain Res* **1609**, 63–71.

Yu LC, Shih YA, Wu LL, Lin YD, Kuo WT, Peng WH, Lu KS, Wei SC, Turner JR & Ni YH (2014). Enteric dysbiosis promotes antibiotic-resistant bacterial infection: systemic dissemination of resistant and commensal bacteria through epithelial transcytosis. *Am J Physiol Gastrointest Liver Physiol* **307**, G824–G835.

Yu LC, Flynn AN, Turner JR & Buret AG (2005). SGLT-1-mediated glucose uptake protects intestinal epithelial cells against LPS-induced apoptosis and barrier defects: a novel cellular rescue mechanism? *FASEB Journal* **19**, 1822–1835.

Yu LC, Huang CY, Kuo WT, Sayer H, Turner JR & Buret AG (2008). SGLT-1-mediated glucose uptake protects human intestinal epithelial cells against *Giardia duodenalis*-induced apoptosis. *Int J Parasitol* **38**, 923–934.

Zhang DW, Shao J, Lin J, Zhang N, Lu BJ, Lin SC, Dong MQ & Han J (2009). RIP3, an energy metabolism regulator that switches TNF-induced cell death from apoptosis to necrosis. *Science* **325**, 332–336.

Additional information

Competing interests

The authors declare that they have no competing interests.

Author contributions

All experiments were performed in the Graduate Institute of Physiology in National Taiwan University, except for liposome preparation performed in the Department of Biochemical Science and Technology, electromicroscopic imaging performed in the Graduate Institute of Anatomy and Cell Biology, and magnetic resonance imaging performed in the Department of Medical Imaging. LCY and CYH were resposible for study concepts and design. CYH, WTK, CYH and WHP were responsible for data acquisition. CYH, TCL, KSL and LCY were responsible for data analysis and interpretation. CYH was responsible for statistical analysis. TCL, CTC and CYY were responsible for material and technical support. All authors were responsible for drafting or revision of the manuscript for important intellectual content, literature research and manuscript editing. All authors have approved the final version of the manuscript and agree to be accountable for all aspects of the work. All persons who qualify for authorship are listed.

Funding

The present study was supported by grants from the Ministry of Science and Technology (102-2628-B-002-009-MY3, 102-2811-B-002-104, 103-2811-B-002 -060) and National Taiwan University (10R7807 and NTU-CDP-105R7798).

Acknowledgements

We thank the staff of the imaging core at the First Core Labs, National Taiwan University College of Medicine, for technical assistance.